Extraction of electrical mechanisms of low-dielectric constant material MSZ for interconnect applications

T.C. Chang[a,e,]*, S.T. Yan[b], P.T. Liu[c], Z.W. Lin[b], H. Aoki[d], S.M. Sze[b,c]

[a]*Department of Physics and Institute of Electronics, National Sun Yat-Sen University, 70 Lien-hai Rd., Kaohsiung 80424, Taiwan, ROC*
[b]*Institute of Electronics, National Chiao Tung University, Hsin Chu, Taiwan, ROC*
[c]*National Nano Device Laboratory, 1001-1 Ta-hsueh Rd., Hsin Chu 30050, Taiwan, ROC*
[d]*Life Science and Electronic Chemicals Division, Clariant Corp., Bunkyo Green Court, 2-28-8 Honkomagome, Bunkyo-ku, Tokyo 113-8662, Japan*
[e]*Center for Nanoscience and Nanotechnology, National Sun Yat-sen University, 70 Lien-hai Rd., Gushan Chiu, Kaohsiung, Taiwan 804, ROC*

Abstract

In this paper, electrical characterization of low-k dielectric methyl-silsesquiazane (MSZ) is presented. Thermal stress and bias temperature stress (BTS) were utilized to evaluate the impact of Cu penetration on dielectric properties. In the investigation of thermal stress performed by furnace annealing, the leakage mechanism of Al- and Cu-gate MIS capacitors is competed by the decrease of the interfacial states between metal and dielectric and the increase of defects resulted from Cu penetration. Also, the leakage conduction mechanism at high electric field is deduced from Schottky emission in conjunction with space-charge-limited current conduction (SCLC) through BTS methods.
© 2003 Elsevier B.V. All rights reserved.

Keywords: MSZ; Low-k; Thermal stress; Bias temperature stress; Schottky emission; Space charge limited current

1. Introduction

When the progress of integrated circuits (ICs) technology continuously scaled down to deep sub-micron regime, the speed of signal propagation is determined by the technology of multi-level interconnection instead of intrinsic transistor delay. The key issues of resistance–capacitance (RC) time delay are related to the wiring metal and the inter-metal dielectrics (IMD). To reduce the resistance and enhance the electromigration reliability, Cu has been recognized as the most suitable alternative for Al as wiring material [1,2]. Besides, low dielectric constant (low-k) materials, instead of traditional silicon dioxide as IMD, are thus inevitable for decreasing the parasitic capacitance. Low-k dielectrics can also alleviate the power consumption and crosstalk between metal lines [3–5]. Low-k dielectric MSZ (Methyl-silsesquiazane), provided by Clariant Corp., whose dielectric constant is ~ 2.6, is methyl-silsesquioxane (MSQ)—like structure derived from methyl-silses-

quioxane. It is a kind of organic polymer and has excellent chemical compatibility and adhesive capability [6]. In this study, we used MSZ as the insulator and Cu as the electrode to research the dielectric degradation caused by Cu penetration. In this work, thermal stress and bias temperature stress (BTS) are utilized to investigate the quality of MSZ against Cu diffusion. Also, the carrier conduction mechanism through MSZ film was identified.

2. Experimental procedure

A metal/insulator/semiconductor (MIS) capacitor structure was used to study the electrical properties of MSZ film. The MSZ solution was spun on the 6-inch Si wafer and pre-baked in air at 150 and 280 °C in sequence, followed by a hydration treatment. It means leaving the sample in cleanroom for 48 h, leading the water to be absorbed on MSZ. The water provides the oxygen to replace the nitrogen elements in methyl-silsesquiazane. From FTIR analyses (not shown), it can be found that the Si–N peaks are gradually reduced and Si–O 'network' grows obviously. Besides, Si–C bonds

---

*Corresponding author. Tel.: +886-3-5726100; fax: +886-3-5713403.

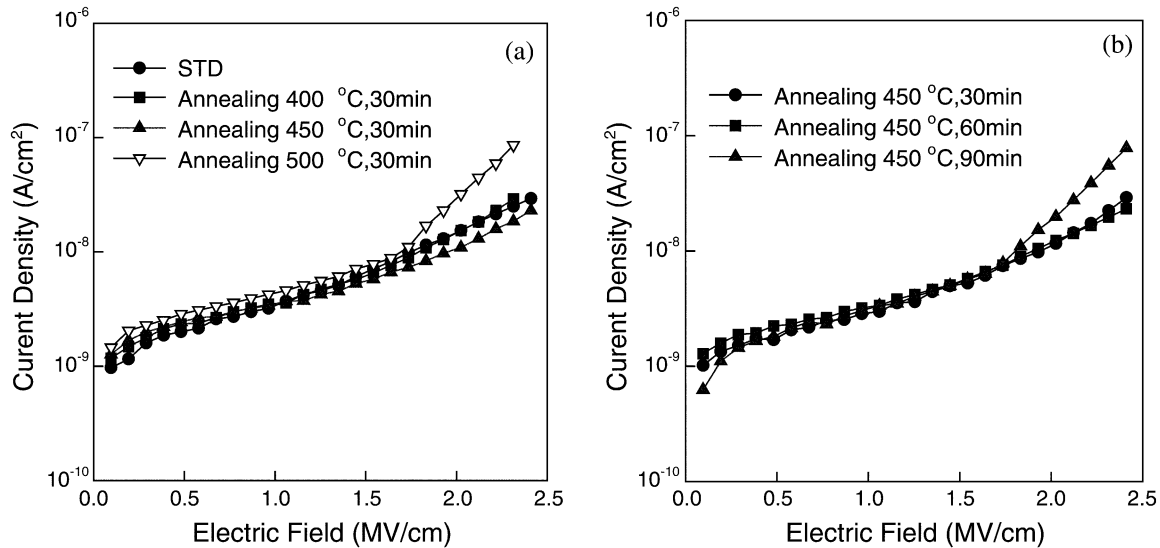*E-mail address:* tcchang@mail.phys.nsysu.edu.tw (T.C. Chang).

Fig. 1. After thermal stress, the current–voltage characteristics with (a) temperature and (b) time dependence for Cu electrode.

gradually grow which determine the quality of MSZ film. Standard MSZ film cannot be formed without hydration process. Subsequently, the coated wafer was cured in a quartz furnace at 400 °C for 1 h under N_2 ambient to remove the residual water. The final MSZ film was formed to a thickness of ~410 nm. Afterward, a 500-nm-thick metal gate Cu was deposited by sputtering and a 50-nm Ti layer was in-situ deposited to prevent the Cu gate from oxidation. Also, Al gate was deposited, without capping Ti layer, in contrast with Cu-gate samples. In our study of thermal stressing, different conditions such as various temperatures and periods of time were performed in a quartz furnace. In addition, two strict BTS conditions were performed on Cu-gate

samples. They were positively biased at 1 and 2 MV/cm both at 170 °C for 1000 s in order to drive the Cu ions in. The current–voltage ($I–V$) characteristics were measured at accumulation mode. During the measurement, N_2 gas is continually purged into the probe station avoiding the moisture absorption and oxidation of Ti. The electrical measurements were performed using a semiconductor parameter analyzer model HP4156.

3. Results and discussions

3.1. Effects of thermal stress

Figures 1 and 2 show the temperature and time-dependent current–voltage characteristics after thermal
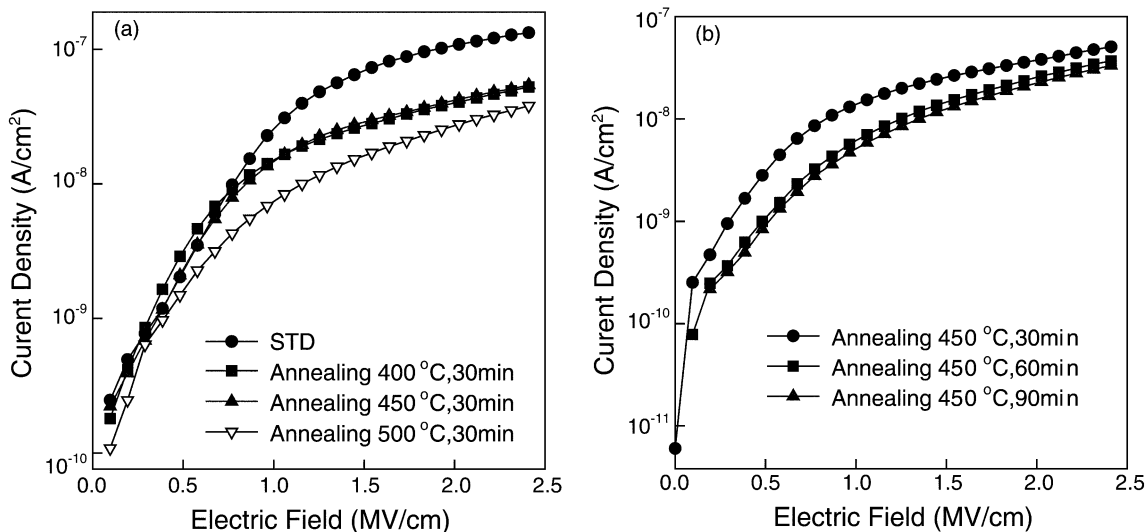

Fig. 2. The current–voltage characteristics with (a) temperature and (b) time dependence for Al electrode.
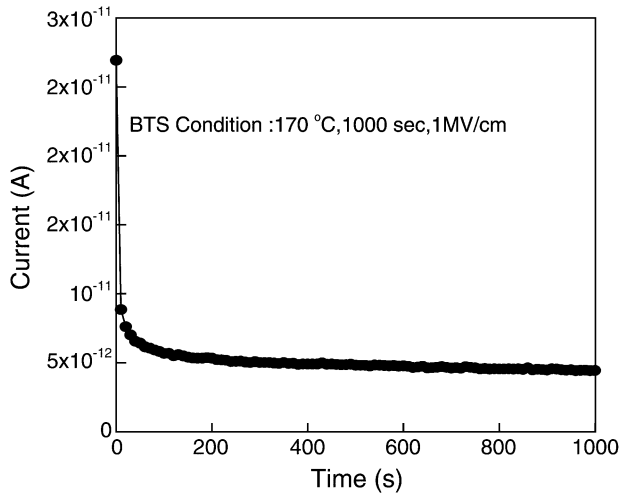
Fig. 3. Current–Time (*I–t*) relation of MSZ during BTS stress.

stress for Cu and Al-electrode capacitors, respectively. As shown in Fig. 1, the leakage current is slightly increased with the elevated temperatures and periods of time. However, quite the other way was observed for Al-electrode samples. It can be deduced that there are two mechanisms competing with each other in the thermal stressing. When the periods of stressing time and temperatures are increased, the defects and interface states may be increased due to thermal drive-in of metal ions [7] or be decreased due to thermal annealing of the interface between metal and MSZ film. Increased temperature and time improves the interface due to repair of discontinuous dangling bonds and the leakage current

is decreased for Al-gate samples. However, thermal drive-in of Cu gate may cause damage or interface states. The results exhibit that the interface between Al electrode and MSZ will be improved and the thermal stress will not cause any damage through the MSZ films even if at 500 °C. For considering the Cu-gate MSZ capacitors, the thermal annealing effect cannot compete with the damage resulted from Cu diffusion. Therefore, the leakage current is increased with annealing time and temperatures. Fortunately, the increased leakage current caused by thermal stress is slight. It is concluded that MSZ can meet the tolerance of the subsequent thermal processes during interconnect manufacturing.

3.2. Effects of bias temperature stress (BTS)

First, we performed a BTS measurement on Cu-gate samples at 170 °C for 1000 s under 1 MV/cm. The current–time (*I–t*) characteristic is shown in Fig. 3. A sharp downward region before saturation is found which means it is hard for copper ions to penetrate into MSZ. Fig. 4 shows the *J–E* curves of Cu-gate capacitors measured at elevated temperatures before and after BTS. The leakage current arises with temperatures as a result of thermal excitation of energetic electrons. Compared with Fig. 4, Fig. 5 shows that MSZ film is so stubborn that the leakage currents are almost the same before and after BTS. This indicates that MSZ is resistant to Cu penetration. A stricter BTS measurement at 2 MV/cm and 170 °C for 1000 s were further performed to investigate the endurance of MSZ, as shown in Figs. 6 and 7. It is found that the leakage current is slightly
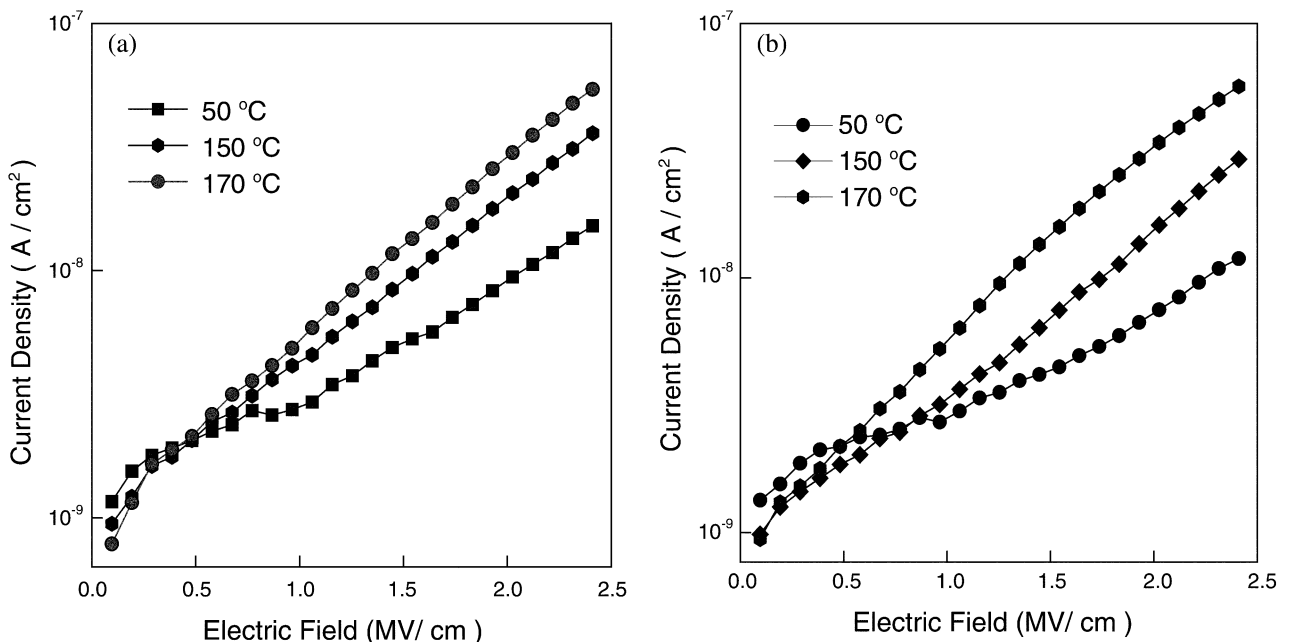

Fig. 4. The leakage current measured with elevated temperatures (a) before and (b) after BTS condition 1000 s, 170 °C and 1 MV/cm.
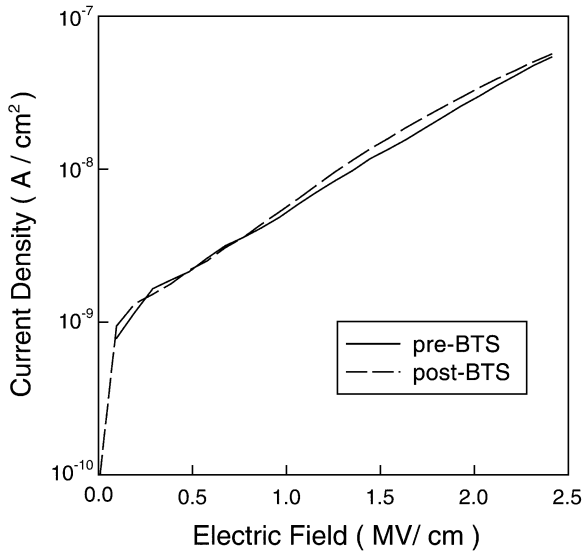
Fig. 5. The *J–E* curve of MSZ measured at 170 °C pre- and post-BTS. The BTS condition is 1000 s, 170 °C and 1 MV/cm.

increased after the stricter BTS condition. Fig. 8 shows a slight increase of leakage current among the saturation region. It is known that there are some traps within the dielectric film. When a continuous electric field is biased for a period of time, the injecting electrons will be captured by the traps, which forms a repulsive electric field. As time passes by, the repulsive electric field will repel the injecting electrons, which leads to the transient decrease of leakage current. Eventually, the steady state causes the saturation region of *I–t* characteristic as Fig. 3. In Fig. 8, it can be inferred that the damage caused during the BTS measurement may lead to the slight
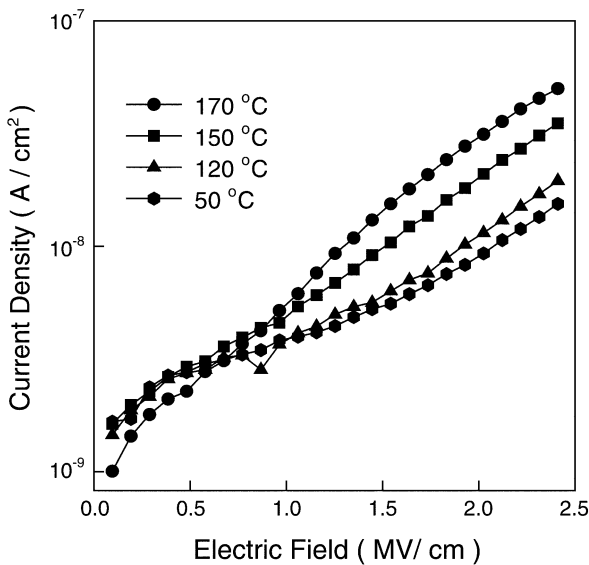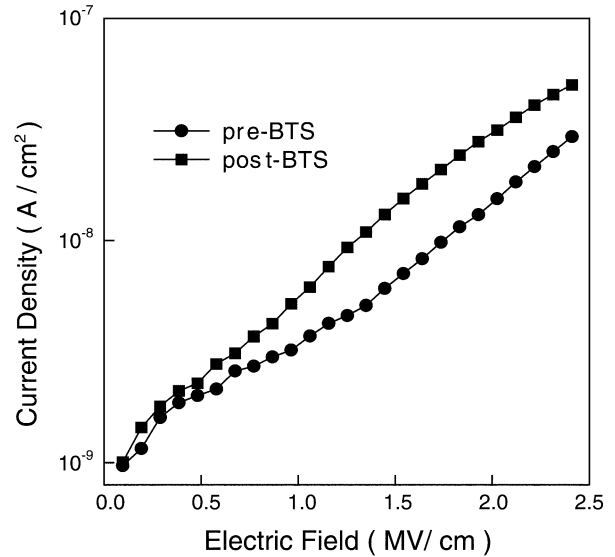

Fig. 7. The *J–E* curve of MSZ measured at 170 °C pre- and post-BTS picked from Fig. 4a and Fig. 6. The BTS condition is 1000 s, 170 °C, and 2 MV/cm.

increase of leakage current in the saturation region. The damage can either be impact ionization due to injected electrons or bond breakage of MSZ due to Cu ion drift. If the damage is continuously increased, it may finally lead to breakdown.

3.3. Carrier conduction mechanism

In the analysis of carrier conduction mechanism, it is found that the leakage current density at high electric field is linearly related to the square root of the applied electric field for all experimental results of pre- and
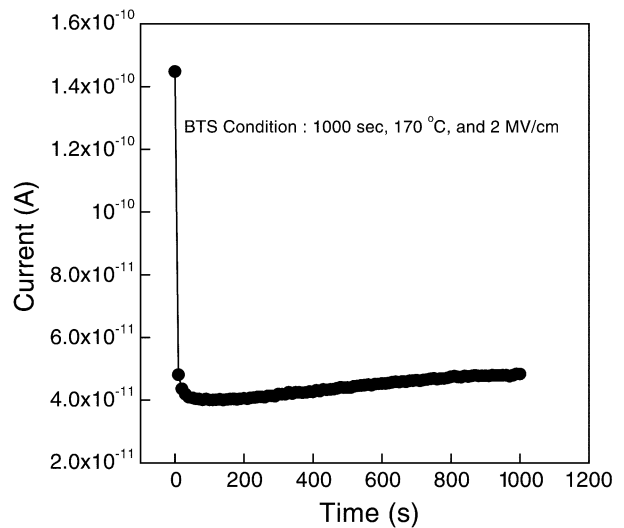

Fig. 6. The leakage current measured with elevated temperatures after BTS condition 1000 s, 170 °C and 2 MV/cm.

Fig. 8. *I–t* characteristic of MSZ during BTS stress. A slight rise of the leakage current is observed.
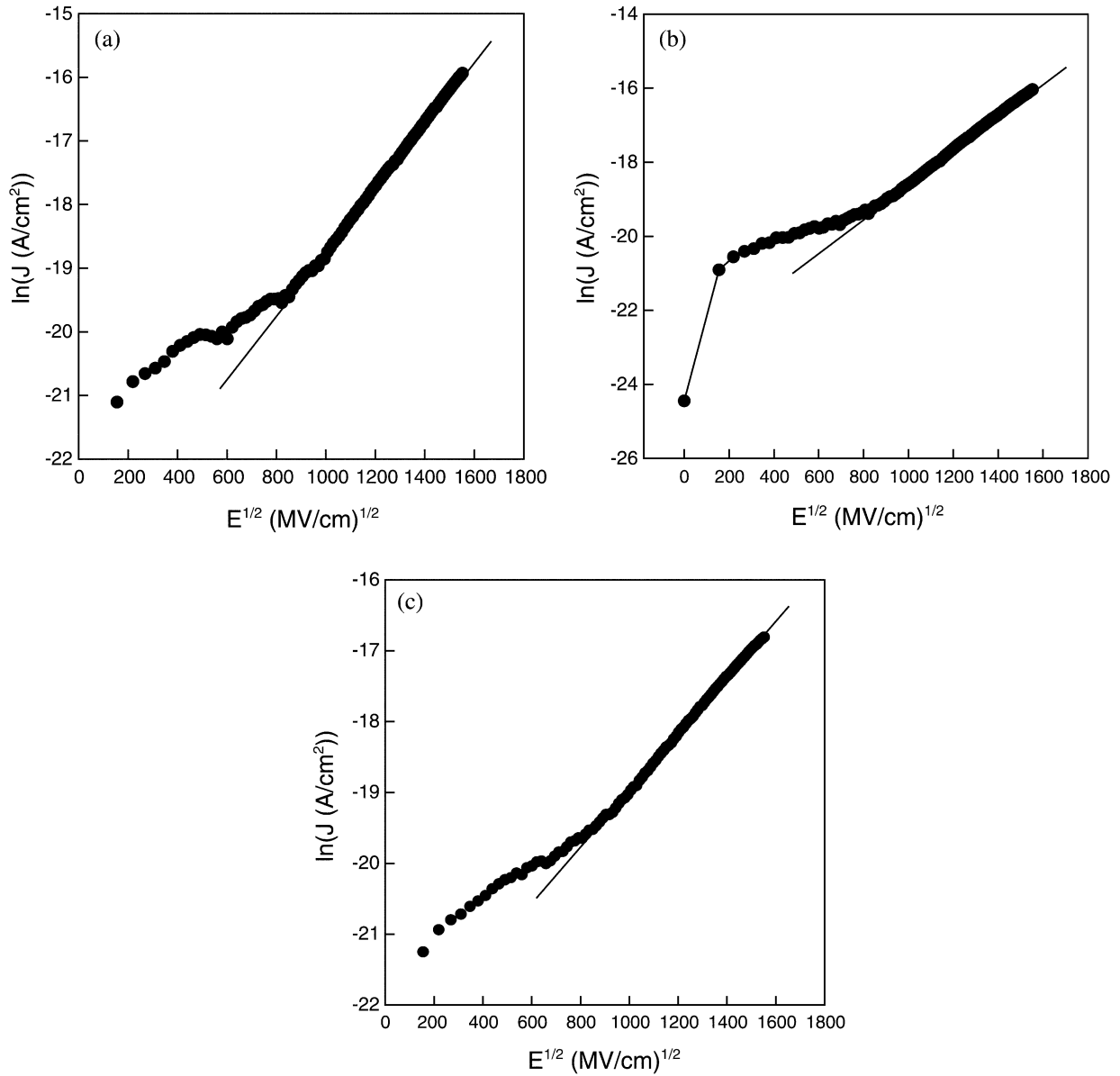
Fig. 9. ln J–$E^{1/2}$ characteristics of (a) pre-BTS (b) post-BTS of condition 1000 s, 170 °C, and 1 MV/cm, and (c) post-BTS of condition 1000 s, 170 °C, and 2 MV/cm measured at 170 °C.

post-BTS conditions shown in Fig. 9. The linear variation of the current corresponds to either Schottky emission or Poole–Frenkel (P–F) emission [7,8]. The current density in the Schottky emission can be quantified by the following equation:

$$J = A^* T^2 \exp\left(\frac{\beta_s E^{1/2} - \phi_s}{k_B T} \right) \qquad (1)$$

where $\beta_s = (e^3/4\pi\varepsilon_0\varepsilon)^{1/2}$, e the electronic charge, ε_0 the dielectric constant of free space, ε the high frequency relative dielectric constant, A^* effective Richardson constant, T absolute temperature, E the applied electric field, ϕ_s the contact potential barrier, and k_B is the

Boltzmann constant. The current density of P–F emission is given by

$$J = J_0 \exp\left(\frac{\beta_{PF} E^{1/2} - \phi_{PF}}{k_B T} \right) \qquad (2)$$

where $J_0 = \sigma_0 E$ is the low-field current density, σ_0 the low-field conductivity, $\beta_{PF} = (e^3/\pi\varepsilon_0\varepsilon)^{1/2}$, and ϕ_{PF} is the height of trap potential well. From the above description we know that β values depend on dielectric constant of the material. For MSZ ($k \sim 2.6$) we calculated that the theoretical β_S and β_{PF} are 3.76×10^{-23} J cm$^{1/2}$V$^{1/2}$ and 7.53×10^{-23} Jcm$^{1/2}$V$^{1/2}$, respectively. In Fig. 9, the experimental β values, extracted from the
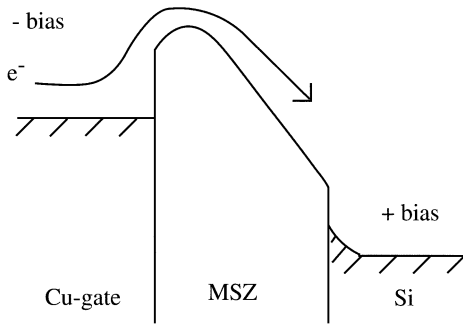
Fig. 10. The band diagram of Schottky emission path for a MIS capacitor.

slope of the linear region (slope$\times k_B T$), are, respectively, 3.13×10^{-23} Jcm$^{1/2}$V$^{1/2}$, 2.51×10^{-23} Jcm$^{1/2}$V$^{1/2}$ and 2.85×10^{-23} Jcm$^{1/2}$V$^{1/2}$ for Fig. 9a, b and c. The β values are smaller than 3.76 and closer to 3.76 than 7.53. It is worth noticing that the experimental β values are smaller than the theoretical ones. As shown in Fig. 10, the band diagram of Schottky emission path for a MIS capacitor is exhibited. It can be deduced that the carrier conduction mechanism should be Schottky emission at high field. The electrons first have to cross the potential barrier built at the interface between metal and insulator and then go through the insulator along the potential difference within the insulator. From Eq. (1), smaller β value leads to smaller leakage current. Consequently, the measured leakage currents are smaller than those calculated from ideal β value. Since the leakage current is reduced, it can be inferred that the conductive electrons must be retarded in the insulator layer after they cross the potential barrier. In Fig. 11, the *I–V* characteristics were measured with MIS capacitors biased at accumulation mode. From 0 to −100 V is repeatedly swept. The *I–V* characteristics with different sweeping times for Cu-gate samples are shown. The leakage current is decreased with the sweeping times and finally approached saturation without decrease. It shows there might exist some charge trapping sites within the insulator and the electrons will be captured to form a local field and retard the other injecting electrons. This kind of conduction mechanism is similar to space-charge-limited current conduction (SCLC). As considering the space-charge-limited current conduction, [9,10] the current density *J* can be expressed as the following equation,

$$J = \frac{9\varepsilon_0\varepsilon_r\mu\theta V^2}{8d^3} \propto E^2 \tag{3}$$

where μ is the free carrier mobility, ε_0 the permittivity of free space, ε_r the relative dielectric constant of the sample material, d the sample thickness, and θ is the ratio of the free charge carriers to trapped ones. Fig. 12,
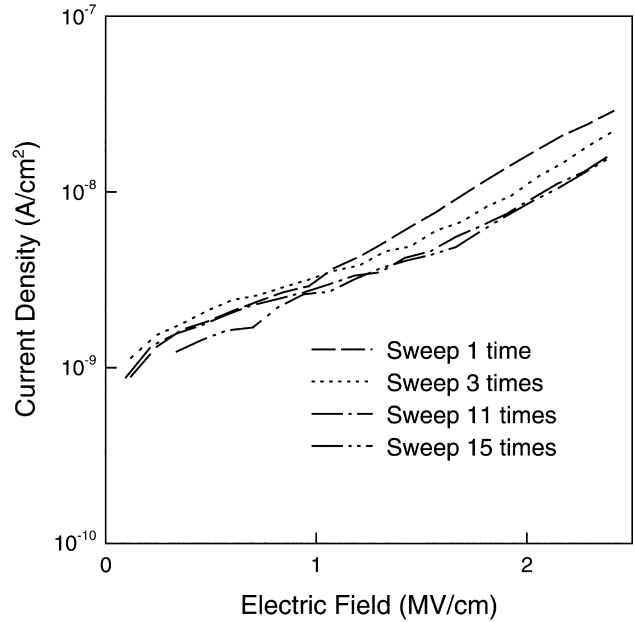

Fig. 11. *J–E* curves performed with different sweeping times. It is found that the leakage current is decreased with increasing sweeping times.

transformed from Fig. 7, shows a linear region at high field. It indicates that *J* is linearly proportional to E^2 at high electric field, which obey the SCLC conduction. Interestingly, among the conduction mechanism of Schottky emission, SCLC conduction also appeared at high field. It is deduced that higher electric field may cause the band bending of the potential barrier, which leads more electrons to be injected into the insulator, and consequently SCLC becomes more pronounced. In
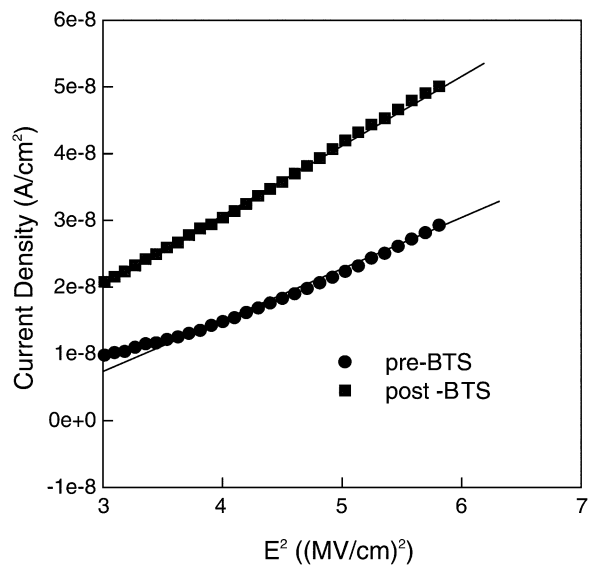

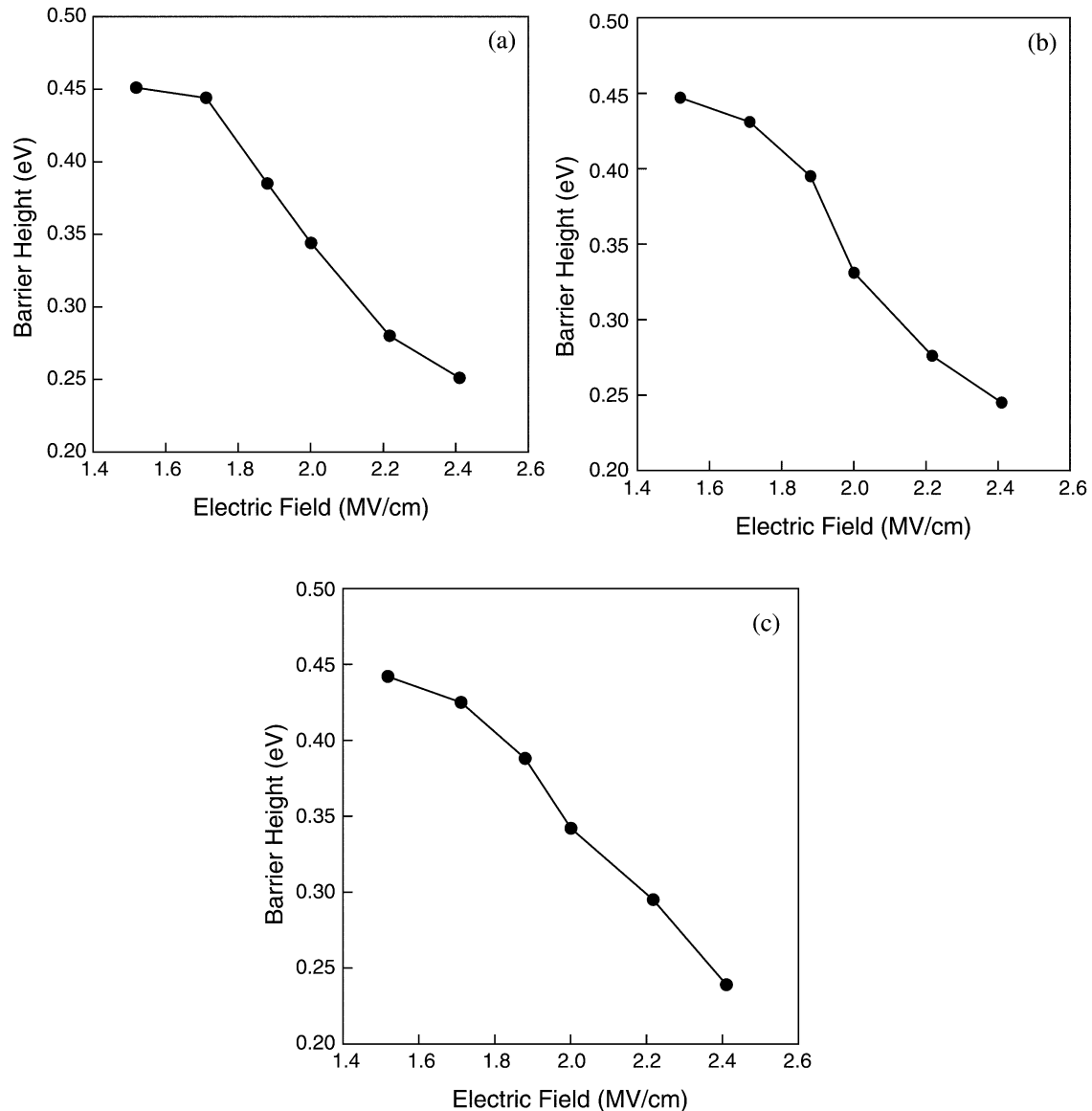Fig. 12. *J–E²* characteristic of MSZ with Cu electrode measured at 170 °C.

Fig. 13. The dependence of effective barrier height vs. electric field for (a) before BTS, (b) after BTS condition 1 MV/cm, and (c) after BTS condition 2 MV/cm.

the high electric field regime, strong injection of excessive electrons occurs and the quasi-Fermi level moves through an appreciable range toward the conduction band [11] Fig. 13, calculated from Fig. 9, exhibits the characteristics of effective barrier height ($\phi_{eff} = \phi_s - \beta_s E^{1/2}$) vs. the electric field. It shows the barrier bends more with the increasing electric field. Under this situation, the requirement for SCLC conduction is achieved. Fig. 14 shows the band diagram for our discussions. In mathematical analyses, the form of the leakage current at high field can be described as the form of SCLC $J \sim E^2$, which approximates to $J \sim \exp(E^{1/2})$ of Schottky emission when Schottky emission is Taylor expanded and the square term is dominant.

That's the cause of coexistence of Schottky emission and SCLC conduction at high field and can be predicted that as the field is higher and higher, without breakdown, SCLC will be more pronounced. From the above analyses, it is concluded that the carriers first surmount the potential barrier between the metal gate and the dielectric by Schottky emission and then are limited by SCLC within the bulk of the dielectric. These two independent conduction mechanisms dominate the conduction mechanism of MSZ at high electric field.

4. Conclusions

In this paper, the electrical characterization of low-*k* dielectric MSZ has been investigated. Thermal stress
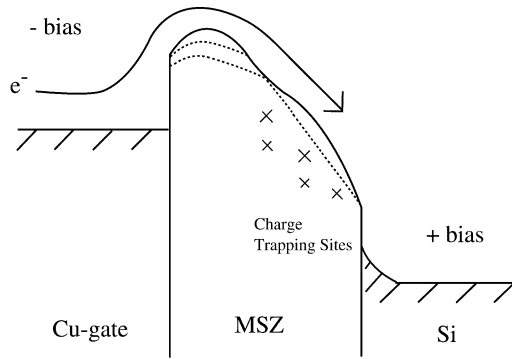
Fig. 14. The band diagram used in our discussion when we performed the electrical measurements.

and bias temperature stress were performed to study the electrical properties and quality of MSZ films. In the research of thermal stress, the leakage current won't be severely degraded for both Cu and Al-electrode capacitors. Also, the carrier conduction mechanism is identified. From the evidence, it is concluded that the carrier conduction mechanism of MSZ is dominated by Schottky emission in conjunction with space-charge-limited current conduction at high field. It is concluded that MSZ is a reliable low-*k* dielectric, which can be used in the Cu-interconnect structure.

References

[1] N. Awaya, H. Inokawa, E. Yamamoto, Y. Okazaki, M. Miyake, Y. Arita, T. Kobayashi, IEEE Trans. Electron. Devices 39 (1996) 1206–1212.
[2] J. Tao, N.W. Cheung, C. Hu, IEEE Electron. Devices Lett. 14 (1993) 249–251.
[3] S. Bothra, B. Rogers, M. Kellam, C.M. Osburn, IEEE Trans. Electron. Devices 40 (1993) 591–597.
[4] S. Wolf, R.N. Tauber, Silicon Processig for the VLSI Era (II), Lattice, Sunset Beach, CA, 1986, pp. 181–199.
[5] T. Sakurai, IEEE Trans. Electron. Devices 40 (1993) 118–124.
[6] Allied Signal Advanced Materials, Accuspin 418 Flowable Spin-on Polymer (SOP), Product Bulletin, Sunnyvale, CA 1996.
[7] P.T. Liu, T.C. Chang, Y.L. Yang, Y.F. Cheng, S.M. Sze, IEEE Trans. Electron. Devices 47 (2000) 1733–1739.
[8] S.M. Sze, Physics of Semiconductor Devices, Wiley, New York, 1981, pp. 402–403, Chap. 7.
[9] T. Iqbal, C.A. Hogarth, Int. J. Electron. 61 (1986) 555.
[10] T. Iqbal, C.A. Hogarth, Int. J. Electron. 65 (1988) 953.
[11] K.D. Mackenie, P.G. Lecomber, W.E. Spear, Philos. Mag. B 46 (1982) 377.